

Exact solution of a lattice model of flux lines in superconductors

H.Y. Huang and F.Y. Wu

Department of Physics, Northeastern University, Boston, MA 02115, USA

We consider a statistical mechanical model describing flux lines in type II superconductors by embedding the flux lines on a lattice wound on torus. The lines are nonintersecting and each loop of lines is associated with a fugacity $z = -1$. It is shown that the exact solution of this model leads to a second-order transition between the Meissner and the superconducting states as well as a first-order transition between the superconducting and the normal states.

1. Introduction

The discovery of high- T_c superconductors has made it possible to experimentally realize fluctuations of flux lines in type II superconductors^{#1}. Flux lines in a superconductor are nonintersecting vortex filaments which wander around in the specimen. The essence of this physical picture can be adopted in a model in which lines are embedded on a lattice and interact with hard-core interactions. This leads to a model of directed lines [2,3] which has been analyzed in the past by the mean-field [4], path-integral [5] and renormalization-group [2] approaches. However, it has not been possible to carry out a first-principle study by solving the model exactly. In this paper we report results of such an analysis.

We study the statistical mechanics of flux lines by applying the exact solution of a related three-dimensional vertex model [6]. Our analysis leads to a description of the thermodynamics and phase diagrams which resembles those of experimental findings.

2. Formulation

We consider flux lines in type II superconductors as directed lines embedded

^{#1} For a review of a statistical mechanical discussion and some relevant experimental facts, see [1].

on a lattice which run along a preferred direction, say the z direction. For definiteness consider a simple cubic lattice whose main diagonal points in the positive z -direction, with all directed lines making 45° angles with the positive z -axis. Assuming periodic boundary conditions, the lines will then form cycles after looping around the lattice one or more times in the z -direction. To each line segment joining two nearest neighbors of the lattice, we associate a line segment energy ϵ . Furthermore, under the presence of an external magnetic field, a line segment in the i th direction, $i = 1, 2, 3$, is associated with a magnetic energy $-H_i$, where H_i is the component of the magnetic field in the i th direction. This leads to the line segment Boltzmann factor,

$$z_i = e^{-\beta(\epsilon - H_i)}, \quad (1)$$

where $\beta = 1/kT$. To each cycle of lines we further associate a fugacity y and consider the partition function

$$Z(y; z_1, z_2, z_3) = \sum_{\text{line config. cycles}} \prod \left(y \prod z_i \right), \quad (2)$$

where the first product is over all cycles of lines and the second product over all lattice edges in a given cycle.

It is straightforward to extend the model (2) to arbitrary d dimensions with, of course, the physical situation described by $d = 3$ and $y = 1$. The $y = 1$ and $y = -1$ models can both be solved exactly in $d = 2$, and the solutions turn out to be identical in the thermodynamic limit [7]. For $d \geq 3$ the $y = -1$ model has recently been solved [6]. While the $y = 1$ model has remained unsolved for $d \geq 3$, its critical behavior in general is not expected to be much different from that of the $y = -1$ model. Indeed, due to the strong constraint imposed by configurations of directed lines, it is known that the $y = \pm 1$ models in $d \geq 3$ share the same critical temperature and belong to the same universality class [6]. Thus, with nothing better available, we shall use the $y = -1$ solution in the formulation and carry out a first-principle analysis on this basis.

From here on we confine our considerations to $y = -1$, and consider the per-site Gibbs free energy of the superconducting state as given by

$$G_s(T, H) = -\beta^{-1} \lim_{N \rightarrow \infty} \frac{1}{N} \ln Z(-1; z_1, z_2, z_3), \quad (3)$$

where N is the total number of sites of the lattice. Generally, if the Gibbs free energy of a system is $G(T, H)$, the ‘‘per-site’’ magnetic induction and magnetization of the system are, respectively and in appropriate units,

$$B(T, H) = -\partial G(T, H) / \partial H, \quad (4)$$

and

$$M = B - H. \quad (5)$$

In addition, the per-site internal energy and the constant field specific heat are

$$U(T, H) = \frac{\partial[\beta G(T, H)]}{\partial \beta} + HB, \quad (6)$$

and

$$C_H = -T \left(\frac{\partial^2 G}{\partial T^2} \right) = \frac{-1}{T^2} \frac{\partial^2}{\partial \beta^2} [\beta G(T, H)]. \quad (7)$$

For the superconducting states we use G_s for G . For the normal state (of a free electron gas) we have the following expression for the Gibbs free energy:

$$G_n(T, H) = G_0 - \frac{1}{2}\gamma T^2 - \frac{1}{2}H^2, \quad (8)$$

where G_0 , $\gamma > 0$ are constants. The system becomes normal whenever the Gibbs free energy G_n is lower than G_0 . The magnetic induction and the specific heat of the normal state are therefore

$$B = H, \quad C_H = \gamma T. \quad (9)$$

3. The exact solution

The directed line problem (2) can be formulated as a 10-vertex problem on the simple cubic lattice [6]. Place bonds along edges of the lattice with the restriction that there are either no bond or two bonds incident at each site and, when there are two incident bonds, one of the bonds is always along a positive axes direction and the other along a negative direction. Thus, the vertex weights are

$$\omega \begin{cases} = 1 & \text{if there is no bond,} \\ = \sqrt{z_i z_j} & \text{if the two bonds are in directions } i \text{ and } j, \\ = 0 & \text{otherwise,} \end{cases} \quad (10)$$

and we have altogether a $(3^2 + 1) = 10$ nonzero vertex weight and a 10-vertex

model. This vertex model is identical to the directed line model (2) if one further introduces the cycle fugacity y .

The partition function (2) can be evaluated using the vertex model formulation for $y = -1$ [6]. This yields, after introducing (3),

$$-\beta G_s(T, H) = \frac{1}{(2\pi)^3} \int_0^{2\pi} d\theta_1 \int_0^{2\pi} d\theta_2 \int_0^{2\pi} d\theta_3 \ln |z_4 + z_1 e^{i\theta_1} + z_2 e^{i\theta_2} + z_3 e^{i\theta_3}|, \quad (11)$$

where $z_4 \equiv 1$. Carrying out one integration as in ref. [6] after changing variables, if needed, we find

$$\begin{aligned} -\beta G_s(T, H) &= \ln z_m, & T < T_c, \\ &= \frac{1}{(2\pi)^2} \int_{\mathcal{R}} \int \prod_{i \neq m} d\theta_i \ln \left| \sum_{j \neq m} z_j e^{i\theta_j} \right|, & T > T_c, \end{aligned} \quad (12)$$

where \mathcal{R} is the regime

$$\left| \sum_{j \neq m} z_j e^{i\theta_j} \right| > z_m \equiv \max\{z_1, z_2, z_3, z_4\}, \quad (13)$$

and T_c given by

$$z_1 + z_2 + z_3 + z_4 = 2z_m, \quad T = T_c. \quad (14)$$

Clearly, the Gibbs free energy is nonanalytic at T_c .

4. Thermodynamic properties

It is now straightforward to combine the exact solution for G_s with the formulation in section 2 to deduce the thermodynamics of a superconductor. The explicit formulation will depend, however, on the direction of the applied magnetic field which gives rise to different H_i .

Consider first the case that the magnetic field H is applied along the 1 direction so that

$$z_1 = e^{-\beta(\epsilon - H)}, \quad z = z_2 = z_3 = e^{-\beta\epsilon}. \quad (15)$$

It is clear then that the critical condition (14) can be realized in two different ways, namely

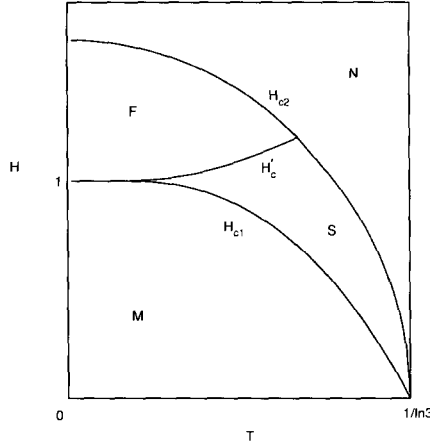


Fig. 1. The phase diagram with H along the 1 direction. M denotes the Meissner state, S the superconducting state, N the normal state, and F the frozen state. H in unit of ϵ and T in unit of ϵ/k .

$$\begin{aligned} z_1 + 2z &= 1, & H &= H_{c1}(T), \\ 1 + 2z &= z_1, & H &= H'_c(T) > H_{c1}. \end{aligned} \tag{16}$$

A plot of the critical conditions (16) is shown in the phase diagram fig. 1. Note that both curves intersect the $T = 0$ axis at $H = \epsilon$, while the $H = H_{c1}(T)$ curve intersects the $H = 0$ axis at

$$T_c = \epsilon/k \ln 3. \tag{17}$$

The system is in a frozen (saturated) state when $H > H'_c(T)$.

The Gibbs free energy (11) can be written in the form [6], after carrying out one or three integrations,

$$-\beta G_s(T, H) \begin{cases} = 0, & H < H_{c1}, \\ = \frac{4}{(2\pi)^2} \int_0^{\theta_0} d\theta \int_0^{\alpha_0(\theta)} d\alpha \ln |z_1 e^{i\alpha} + u(\theta)|, & H_{c1} < H < H'_c, \\ = -\beta(\epsilon - H), & H > H'_c, \end{cases} \tag{18}$$

where

$$\begin{aligned} \cos \frac{1}{2} \theta_0 &= (1 - z_1)/2z, \\ \cos \alpha_0(\theta) &= [1 - u^2(\theta) - z_1^2]/2u(\theta) z_1, \\ u(\theta) &= 2z \cos \frac{1}{2} \theta. \end{aligned} \tag{19}$$

Since the system is frozen with zero free energy and no flux for $H < H_{c1}$, we identify the transition at $H_{c1}(T)$ as the transition to the Meissner state. On the other hand, flux lines become frozen (saturated) for $H \geq H'_c$. However, this frozen transition can be unphysical since the normal state (8) may dominate giving rise to a lower Gibbs free energy. This leads us to consider the transition to the normal state occurring at

$$G_s(T, H) = G_n(T, H), \quad H = H_{c2}(T). \quad (20)$$

We have determined $H_{c2}(T)$ numerically using (20) in conjunction with (18) and (8) and the choice of constants

$$G_0 = \frac{1}{2}\gamma T_c^2, \quad \gamma = 3, \quad (21)$$

where G_0 is chosen to ensure $H_{c2}(T)$ to vanish at T_c , and γ is arbitrary as it does not effect our general conclusion. The resulting $H_{c2}(T)$ is shown in the phase diagram in fig. 1. It is seen that, as commented earlier, the state with saturated magnetic induction for large H is unphysical as it is superceded by the normal state.

It is clear that the transition at H_{c2} between the normal and superconducting states is of first order, since the free energies in the two regimes are given by different analytic expressions. To analyze the nature of transition at H_{c1} , we need to evaluate the internal energy (6). First we evaluate the per-site induction using (4) and (18), obtaining

$$\begin{aligned} B(T, H) &= \frac{1}{\pi^2} \frac{\partial \theta_0}{\partial H} \int_0^{\alpha_0(\theta_0)} d\alpha \ln |z_1 e^{i\alpha} + u(\theta_0)| \\ &+ \frac{1}{\pi^2} \int_0^{\theta_0} d\theta \frac{\partial \alpha_0(\theta)}{\partial H} \ln |z_1 e^{i\alpha_0(\theta)} + u(\theta)| \\ &+ \frac{1}{\pi^2} \int_0^{\theta_0} d\theta \int_0^{\alpha_0(\theta)} d\alpha \frac{z_1 z'_1 + u z'_1 \cos \alpha}{u^2 + z_1^2 + 2u z_1 \cos \alpha}, \end{aligned} \quad (22)$$

where $z'_1 = \partial z_1 / \partial H = \beta z_1$. Using the integration formula

$$\int_0^{\phi_0} d\phi \frac{A + B \cos \phi}{a + b \cos \phi} = \frac{B}{b} \phi_0 + \frac{Ab - aB}{b} \frac{2}{\sqrt{a^2 - b^2}} \tan^{-1} \left(\sqrt{\frac{a-b}{a+b}} \tan(\frac{1}{2} \phi_0) \right) \quad (23)$$

and after some algebra, we find

$$B(T, H) \begin{cases} = 0, & H < H_{c1}, \\ = \frac{1}{2\pi^2} \int_0^{\theta_0} d\theta \left[\alpha_0(\theta) - 2 \tan^{-1} \left(\frac{u(\theta) - z_1}{u(\theta) + z_1} \tan \left[\frac{1}{2} \alpha_0(\theta) \right] \right) \right], & H_{c1} < H < H'_c, \\ = 1, & H > H'_c. \end{cases} \quad (24)$$

In a similar fashion we evaluate $U(T, H)$ using (6) and $B(T, H)$ given by (24). This leads to the surprisingly simple expression

$$U(T, H) \begin{cases} = 0, & H < H_{c1}, \\ = \frac{\epsilon}{\pi^2} \int_0^{\theta_0} d\theta \alpha_0(\theta), & H_{c1} < H < H'_c, \\ = \epsilon, & H > H'_c. \end{cases} \quad (25)$$

Results of numerical evaluation of $U(T, H)$ are shown in fig. 2. It can be shown that both $B(T, H)$ and $U(T, H)$ are continuous at H_{c1} and H'_c . To determine the nature of transition, we compute the specific heat using (7) and obtain, after some algebra,

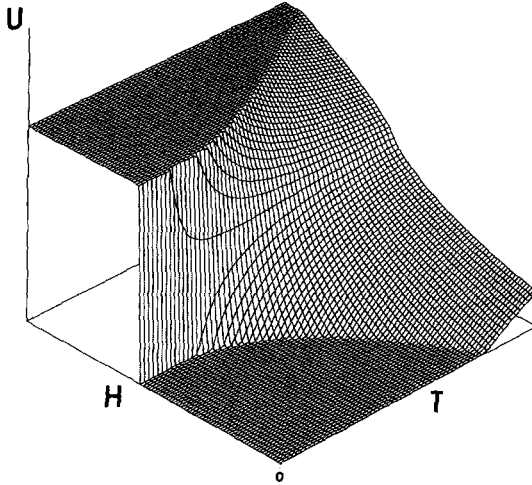


Fig. 2. The internal energy $U(T, H)$ given by (25) with H along the 1 direction.

$$C_H \begin{cases} = 0, & H < H_{c1}, \\ = \frac{2}{\pi^2 k T^2} \int_0^{\theta_0} d\theta \frac{\csc \alpha_0(\theta)}{2u(\theta) z_1} \{ \epsilon^2 - \epsilon H [1 - u^2(\theta) + z_1^2] + H^2 z_1^2 \}, & H_{c1} < H < H'_c, \\ = 0, & H > H'_c. \end{cases} \quad (26)$$

Along the critical lines given by (16), the specific heat C_H has a cusp and assumes the finite value

$$C_H = \frac{(\epsilon - H z_1)^2}{2\pi k T^2 z \sqrt{z_1}}, \quad (27)$$

where $z_1 = 1 \mp 2z$. Particularly, at $H = 0$, we have the critical value

$$C_0 = \frac{3\sqrt{3}}{2\pi} (\ln 3)^2 k. \quad (28)$$

Therefore, the transition at $H_{c1}(T)$ is of second order. A plot of (27) is given in fig. 3.

The above analysis can be carried out for the applied magnetic field assuming arbitrary direction. For the field in the 1-2 plane, for example, we define, in place of (15),

$$z_1 = e^{-\beta\epsilon}, \quad z = z_2 = z_3 = e^{-\beta(\epsilon - H)}. \quad (29)$$

The analysis leads to a *unique* critical condition

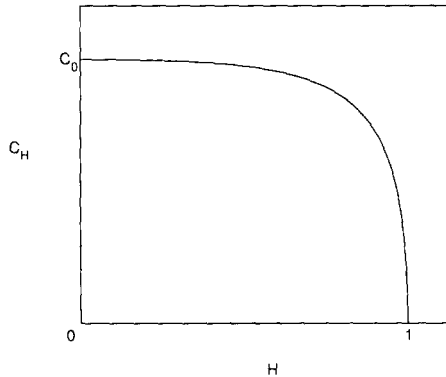


Fig. 3. The critical value of the specific heat C_H along $H = H_{c1}$ along the 1 direction. H in unit of ϵ .

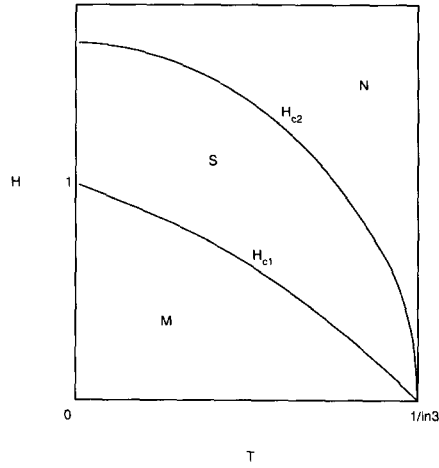


Fig. 4. The phase diagram with H in the 1-2 direction. M denotes the Meissner state, S the superconducting state, and N the normal state.

$$2z + z_1 = 1, \quad H = H_{c1}(T). \tag{30}$$

Thus, the frozen saturated state does not appear. A plot of (30) is given in the phase diagram shown in fig. 4.

We can similarly compute the energy and the specific heat, except that there is now no critical field $H'_c(T)$. Using the energy $U(T, H)$ given by the first two lines in (25), we obtain the specific heat

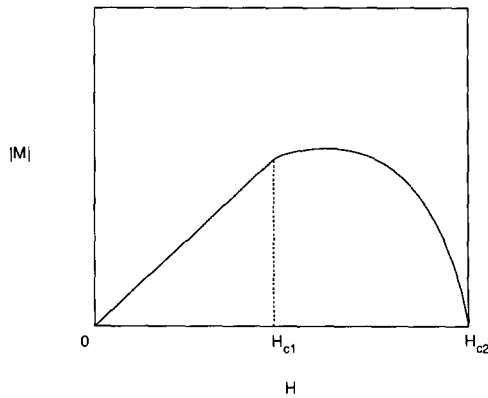


Fig. 5. The magnetization M as a function of H at $T = 0.8T_c$. H in unit of ϵ and T in unit of ϵ/k .

$$C_H \begin{cases} = 0, & H < H_{c1}, \\ = \frac{2}{\pi^2 k T^2} \int_0^{\theta_0} d\theta \frac{\csc \alpha_0(\theta)}{2u(\theta) z_1} \{ \epsilon^2 - \epsilon H [1 + u^2(\theta) - z_1^2] + H^2 u^2(\theta) \}, & H > H_{c1}. \end{cases} \quad (31)$$

Along the critical line $H = H_{c1}(T)$ given by (30), the specific heat C_H again has a cusp and assumes the value

$$C_H = \frac{(\epsilon - 2Hz)^2}{2\pi k T^2 z \sqrt{z_1}}, \quad (32)$$

with C_0 again given by (28). Note the remarkable resemblance of (31) and (32) with (26) and (27). However, the expression (32) diverges as $e^{\beta\epsilon/2}$ at $\{H, T\} = \{\epsilon, 0\}$.

Finally, one can compute the per-site magnetization M using (5). The plot of $|M|$ as a function of H for $T = 0.8T_c$, for example, is shown in fig. 5.

Acknowledgements

We are indebted to T. Hwa and R.S. Markiewicz for useful discussions. This work is supported in part by NSF Grants DMR-9015489, DMR-9313648 and INT-9207261.

References

- [1] D.R. Nelson, J. Stat. Phys. 57 (1989) 511.
- [2] S.M. Bhattacharjee and J.J. Rajasekaran, Phys. Rev. A 44 (1991) 6202.
- [3] D.R. Nelson and H.S. Seung, Phys. Rev. B 39 (1989) 9153;
D.R. Nelson, Phys. Rev. Lett. 60 (1988) 1973.
- [4] T. Izuyama and Y. Akutsu, J. Phys. Soc. Jpn. 51 (1982) 50.
- [5] S.M. Bhattacharjee, Europhys. Lett. 15 (1991) 815.
- [6] F.Y. Wu and H.Y. Huang, Lett. Math. Phys. 29 (1993) 205.
- [7] P.W. Kastelyn, Physica 27 (1961) 1209.